Materials Research. 2018; 21(1): e20170012
DOI: http://dx.doi.org/10.1590/1980-5373-MR-2017-0012

Effect of LZSA Glass-Ceramic Addition on Pressureless Sintered Alumina. Part II: Mechanical Behavior

Oscar Rubem Klegues Montedo[a]*, Pâmela Cabreira Milak[a], Cristian Arnaldo Faller[a], Michael Peterson[a], Agenor De Noni Junior[a]

[a]Universidade do Extremo Sul Catarinense - UNESC, Avenida Universitária, 1105, Criciúma, SC, Brazil

Received: January 06, 2017; Revised: August 19, 2017; Accepted: September 17, 2017

This work aims to evaluate the influence of a Li_2O-ZrO_2-SiO_2-Al_2O_3 (LZSA) glass-ceramic on the mechanical behavior of alumina. Composites were prepared from alumina with three different particle sizes and 7 to 21 vol% of an LZSA glass-ceramic composition ($11.6Li_2O$-$16.8ZrO_2$-$68.2SiO_2$-$3.4Al_2O_3$,). Specimens were obtained by uniaxial pressing. The optimum sintering temperature and holding time were found to be different for each composite. Structural characterization (bulk density and crystalline phases); mechanical characterization (flexure strength, elastic modulus, fracture toughness, and fracture energy); and microstructural analyses were carried out. Fine-grained alumina-based composite containing 21 vol% of glass-ceramic (1470 ºC and 3 h holding time, 2.0% porosity) showed a fracture toughness of 4.93 $MPa \cdot m^{0.5}$, an elastic modulus of 210 GPa, a fracture energy of 57 $J \cdot m^{-2}$, and a flexural strength of 170 MPa, in very good agreement with values reported by the literature. An increase of 37-177% in the fracture energy due to 21 vol% LZSA addition in the alumina was achieved for the range of grain size obtained in this work. Even though the final composition included a glassy component, the observed mechanical properties confirmed the effectiveness of the crystalline phases that were formed from LZSA glass-ceramic in reducing the propagation of cracks. The results showed that the addition of the LZSA glass-ceramic improved the mechanical properties of alumina.

Keywords: *Alumina, LZSA glass-ceramic, composites, mechanical behavior*

1. Introduction

Ceramic materials have been used to meet engineering requirements[1], such as high wear-resistance in the power generation and aerospace industry[2,3], because of their essential characteristics, such as chemical stability, fairly high hardness[1-3], lower density when compared to metals[2], high mechanical strength[1,3], good refractory properties[1-4], and high corrosion resistance[2]. Alumina is a typical engineering ceramic[1,5-7] used in structural applications[7]; automotive, aerospace, biomedical, and ballistic applications[8]; and cutting tools[9].

Many studies have shown the influence of microstructure on the mechanical behavior of alumina, and most of them were focused on the effects of grain size[10-17]. A fine-grained microstructure[3,10,11] and narrow range of particle size distribution often result in an improvement of the mechanical behavior of alumina[10,11]. For instance, similar relationships between wear rates and grain size are observed in various wear modes, such as erosive wear, abrasive wear, cutting, and grinding[12]. Moreover, the mechanical strength of alumina may be improved when the microstructure shows fine grain-size and residual porosity less than 0.05%[15].

Solid state sintering contributes to grain growth in alumina, because of the high temperatures and holding times applied. Thus, Liquid Phase Sintering (LPS) has emerged as a feasible alternative to obtain dense alumina with a refined microstructure and low porosity. The LPS application plays an important role in the processing of alumina, because the use of additives during this process allows the formation of a second phase that controls the grain growth phenomena. It seems that the erosive wear rate of LPS alumina is controlled by a combination of different features that may be related to grain size[14]. The types of glass that are most commonly used in LPS contain amorphous silica in their composition, which can degrade the mechanical behavior of the material[18]. Furthermore, the glassy phases are fragile and show low fracture toughness.

A reduction of the residual glassy phase can improve the mechanical behavior of alumina obtained by LPS. Thus, the use of a glass-such as a glass-ceramic-that encourages sintering during heating and also crystallizes in stable phases during the cooling cycle may be an alternative way to obtain high-density alumina by LPS, while simultaneously producing a large amount of crystalline phase in the grain boundaries[19]. In addition, less grain growth and less residual glassy phase could be obtained.

The formed glass-ceramic must have a low coefficient of thermal expansion (CTE) in order to generate compressive residual stress at the interfaces with the alumina. This stress should strengthen the structure, hampering the stripping of

*e-mail: oscar.rkm@gmail.com

alumina grains and improving the mechanical performance of the material. Among the several known glass-ceramic systems, LZSA (Li_2O-ZrO_2-SiO_2-Al_2O_3) crystallizes mostly as β-spodumene$_{ss}$ (solid solution, $Li_2O{\cdot}Al_2O_3{\cdot}4$-$10SiO_2$) and zirconium silicate ($ZrSiO_4$)[20-22], allowing the fabrication of materials with a low CTE (ranging from 5.1 to 5.3 × 10^{-6} °C^{-1}, over the range of 25 to 325 °C)[20]. The high crystallinity, low porosity, and fine microstructure (crystal sizes of 1 μm) that are obtained[21-22] result in high wear resistance and flexural strength[23]. Moreover, LZSA shows surface crystallization and achieves high densification at lower temperatures: above 95% in the range of 630 to 770 °C[22,24].

Alumina-based composites have been studied in order to achieve high performance materials[4-6,8], and it was found that the introduction of a second crystalline phase to improve the properties of alumina, such as fracture toughness, plays an important role. In fact, Montedo et al.[25] studied the effect of the LZSA (11.6Li_2O-16.8ZrO_2-68.2SiO_2-3.4Al_2O_3) glass-ceramic on the grain growth of alumina. The addition of 21 vol% LZSA to fine alumina (d_{50} = 0.5 μm) enabled the lowering of the sintering temperature from 1600 to 1470 °C, and the holding time from 10 h to 40 min, for the same relative density.

Thus, Part II of this work aims to evaluate the effect on the mechanical behavior of alumina caused by the addition of an LZSA glass-ceramic.

2. Experimental

Five compositions were prepared from an LZSA glass-ceramic composition (Tecnofrita, Brazil) and three grades of alumina (99.8 wt% of Al_2O_3, Almatis, USA); the chemical composition, particle size, and specific surface area of these materials were presented in the previous work[25]. The experimental design used two factors: the particle size of alumina and the glass-ceramic content varied on two levels (−1 and +1). A full factorial design 2^2 was established with three central points. The variation ranges of the factors are shown in Table 1. The description A_i is related to the particle size of alumina, where A_F is the fine alumina, A_M is the medium alumina, and A_C is the coarse alumina. The number next to this description refers to the glass-ceramic content. Compositions were wet-mixed (with 0.1 wt% sodium tripolyphosphate as dispersant, 1.0 wt% carboxymethylcellulose as plastifier, and 1.5 wt% polyvinyl alcohol as binder) and dried in a spray-dryer (LabMaq do Brasil Ltda LM MSD 1.0, Brazil) to obtain powders (8 wt% water). The powders were formed by uniaxial pressing (Gabbrielli GT 0785, Italy) at 128 MPa specific pressure with a green density ranging from 1.92 to 2.61 g·cm^{-3}, (i.e., 50.9 to 65.4% of theoretical density) depending on the LZSA content, and dried at 110 ± 5 ºC. The sintering temperature was measured by an optical dilatometer (Expert System Solutions S.R.L Misura HSM ODHT 1400, Italy); and the temperature cycle included a 1 ºC·min^{-1} heating rate, 90 min holding times at 1100 and 1300 ºC, and a 1600 ºC maximum temperature). Sintering temperatures and holding times are shown in Table 1. The compacted alumina and the composites were sintered in an electrical kiln (Fortelab ME 1700/10, Brazil). Controlled cooling (10 ºC·min^{-1} cooling rate, 30 min holding time at 760 ºC, 10 ºC·min^{-1} cooling rate up to room temperature) was carried out in order to form crystalline phases in the glass-ceramic. Porosities were calculated from d_{rel}; the values of which were published by Montedo et al.[25]. The flexural strength (FS) of the sintered samples was determined based on ASTM 1161-02 using a mechanical testing machine (EMIC DL10000, Brazil). The elastic modulus was determined in a transitory vibration analyzer (ATCP Engenharia Física Sonelastic, Brazil). Fracture toughness measurements (K_{IC}) were performed using the notch method (Single Edged Notched Beam, SENB), which consists of making a notch in the specimen by means of a diamond cutting disk (0.8 mm thickness, 0.5 mm pitch). The depth of the notch was equal to 40% of the total thickness of the specimen. Then the specimens were submitted to flexure in a mechanical testing machine (EMIC DL10000, Brazil). The value of K_{IC} was calculated by the Griffith equation:

Table 1. Experimental design with the combinations among each factor.

Material code	d_{50}(μm) of alumina	LZSA		Sintering conditions	
		(vol%)	(wt%)	T (ºC)	t (h)
A_F	0.5	0	0	1600	4
A_M	1.7	0	0	1600	7
A_C	2.8	0	0	1600	10
A_F7	0.5	7	5	1600	4
A_C7	2.8	7	5	1600	7
A_F21	0.5	21	15	1470	3
A_C21	2.8	21	15	1600	0.67
A_M15-1	1.7	15	10	1600	3
A_M15-2	1.7	15	10	1600	3
A_M15-3	1.7	15	10	1600	3

$$K_{IC} = \sigma \cdot Y \cdot \sqrt{a} \quad (1)$$

where σ is the rupture stress, *Y* is the calibration factor and / is the depth of the notch (or the natural flaw).

The calibration factor for this type of notch is given by Eq. 2, where *b* is the width of the specimen.

$$Y = 1.99 - 2.47\left(\frac{a}{b}\right) + 12.97\left(\frac{a}{b}\right)^2 - 23.17\left(\frac{a}{b}\right)^3 + 24.8\left(\frac{a}{b}\right)^4 \quad (2)$$

From the data of K_{IC} and FS measurements, the natural flaw size, *a*, may be calculated from Griffith equation.

According to the theory of fracture mechanics, one can obtain the fracture energy (γ) of the material from Eq. 3, where E is the elastic modulus.

$$K_{IC} = \sqrt{2 \cdot E \cdot \gamma} \quad (3)$$

Five specimens of each condition were used for measurements of mechanical properties.

The residual stress resulting from the interaction between alumina and LZSA was obtained by X-ray diffractometry (Shimadzu XRD-6000, Japan; radiation CuKα, 0.02º step) by means of the evaluation of the displacement in the 2θ angle of the highest α-alumina peak (Bragg's law, 57.47º (116), JCPDS card number 42-1468). The microstructure of the sintered samples was evaluated by scanning electron microscopy (SEM, Zeiss EVO MA10, Germany). Fractured samples were used to assess the interaction between the alumina and the glass-ceramic. Specimens were etched in 2 vol% HF for 25 s and coated with a thin Au film. This chemical etch was carried out to eliminate the glass-ceramic existing on the surface of the samples and thereby allow the visualization of the grain morphology and particles.

3. Results and Discussion

Part I of this work demonstrated the effect of an LZSA glass-ceramic on the grain growth of alumina[25], since the grain size is one of the most important microstructural features that must be controlled in order to obtain high performance alumina. Microstructural control by means of dopants and processing techniques can improve the mechanical properties of alumina-wear for example[16]. Thus, suppression of grain growth plays a crucial role.

In this Part II, LZSA glass-ceramic was added to alumina to cause suppression of grain growth; however, crystalline phases were formed during heating in the range of 640-820 °C[19].

Because the composites were sintered at higher temperatures (> 1450 °C), those crystalline phases were dissolved into the glassy phase after the melting of the LZSA. Nevertheless, after sintering, the controlled cooling of composites allowed the crystallization of LZSA. In fact, Figure 1 shows that β-spodumene$_{ss}$ ($Li_{0-6}Al_{0-6}Si_{2-4}O_6$, JCPDS No. 21-503, and $LiAlSi_3O_8$, JCPDS No. 15-27), zirconium oxide (ZrO_2, JCPDS No. 13-307), and quartz (SiO_2, JCPDS No. 5-490) were formed during the controlled cooling of composite A_F21. Those crystalline phases caused the formation of compressive stress at the alumina/glass-ceramic interface as confirmed by the displacement of the main alumina peak in the XRD patterns[19].

Figure 2 shows the elastic modulus (E) of the alumina ceramics and composites that were investigated in this study, as a function of the LZSA content. One may observe that E shows an inversely proportional behavior in relation

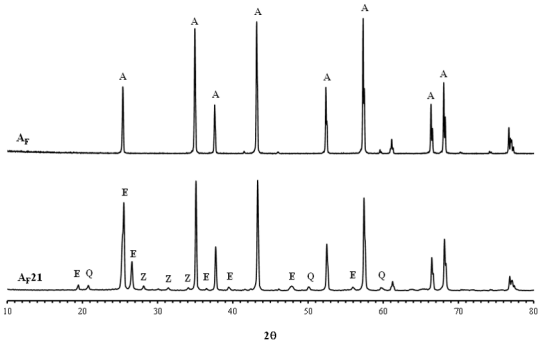

Figure 1. XRD patterns of alumina A_F and composite A_F21. A: Al_2O_3, E: β-spodumene$_{ss}$, Q: quartz (SiO_2), Z: ZrO_2. Alumina A_F was sintered at 1600 ºC (30 min holding time) while composite A_F21 was sintered at 1470 ºC (3 h holding time) and summited to controlled cooling at 760 ºC (30 min holding time).

to porosity. The maximum value in the E-LZSA content plot was obtained at 7 vol% LZSA (94.8% Al_2O_3 purity) regardless of the amount of alumina used (porosity of 5.1 and 4.1% for A_F7 and A_C7, respectively). However, at higher LZSA contents E diminishes probably because of the poor distribution of LZSA into the bulk of alumina. Terheci[26] obtained higher E values for pure alumina compositions (386 GPa, 1600 ºC/30 min holding time), while Munro[27] obtained 416 ±30 GPa for 99.5% purity Al_2O_3 sintered at 1700 ºC and showing 5-µm grain size and 2.0% porosity; the value of E decreased for longer sintering holding times. For the types of alumina used in this study, alumina particle size had no significant effect on the E values for the LZSA compositions that were investigated.

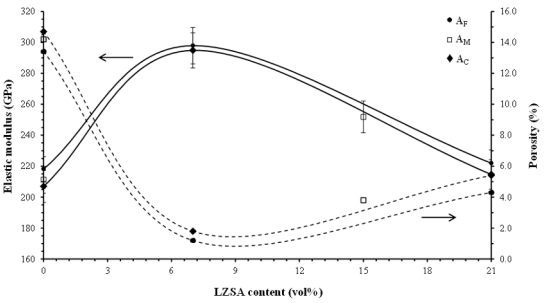

Figure 2. Elastic modulus (E) and porosity in function of the LZSA content of the alumina ceramics and LZSA/alumina composites.

Figure 3 shows K_{IC} results for the alumina ceramics and composites. The LZSA addition increased K_{IC} regardless of the alumina particle size used in this work. The K_{IC} values were found to be 4.24, 4.93, 3.9, and 4.6 MPa·m$^{0.5}$ for A_F7, A_F21, A_C7, and A_C21, respectively. Taking into account the obtained standard deviation, one can say that there is no difference between these K_{IC} values, although one can observe a tendency of K_{IC} increasing for higher values of LZSA content and lower particle sizes. Lube et al.[28] obtained

3.8 MPa·m$^{0.5}$, while Marques[29] cited K_{IC} values ranging from 3.85 to 3.95 MPa·m$^{0.5}$ for sintered alumina (relative density of 99.5%). Tuan et al.[30] found 5.0 MPa·m$^{0.5}$ for sintered alumina (1.7% porosity, 13.3-µm grain size), and Wu et al.[18] found 3.6 MPa·m$^{0.5}$ for pure alumina and 4.8 MPa. m$^{0.5}$ for LPS alumina. Therefore, even though composites A_F7, A_F21, A_C7, and A_C21 had glass in their composition, they showed K_{IC} values larger than those for pure alumina reported for the literature, confirming the effectiveness of the crystalline phases formed from LZSA glass-ceramic to reduce the crack propagation.

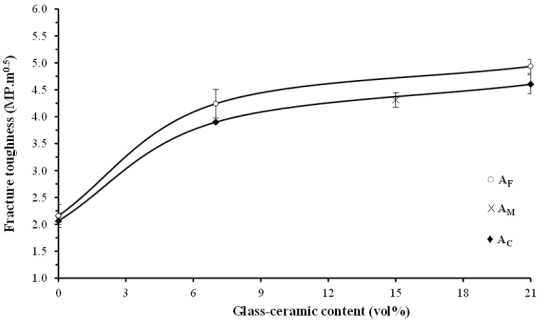

Figure 3. Fracture toughness in function of the LZSA content of the alumina ceramics and LZSA/alumina composites.

Fracture energy (γ) was calculated from the data of K_{IC} and E, using Eq. 3. Figure 4 shows the effect of LZSA content on the fracture energy of alumina. Fracture energy increased with increasing LZSA content for the investigated composites. This effect may be attributed to the alumina/LZSA interaction and the obtained microstructures, in particular, the increase of roughness. However, it is important to emphasize that pure alumina (A_F, A_M, and A_C) were sintered at the same temperature as the composites, i.e. 1600 °C, and because of this, the obtained relative densities were much lower than that of dense alumina. Nevertheless, fracture energy data of alumina with very similar grain sizes and porosities in relation to the investigated composites were obtained from National Institute of Standards and Technology - NIST[31], as shown in Table 2. Table 2 shows that the fracture energy ranges from 18.0 to 36.5 J·m^{-2} for alumina similar to that used in this work. Taking into account that the grain size obtained in this work ranged from ~1 to 12 µm, one may say that the addition of LZSA glass-ceramic increased the fracture energy of alumina up to 50 J·m^{-2} (21 vol% LZSA addition), which represents an increase of 37-177%.

Figure 5 shows images (photographies) of composites A_F7, A_F21, A_C7, and A_C21. The textures of the composites containing 7 and 21 vol% of LZSA are quite different from each other. One can see that the 21-vol% based-composites (A_F21 and A_C21) are much rougher than the 7-vol% based-composites (A_F7 and A_C7). The rougher the material, the greater the contact between particles; consequently, more

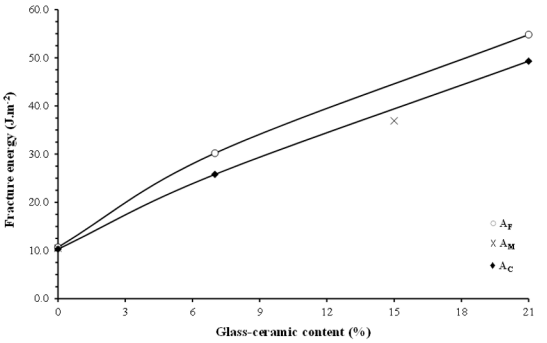

Figure 4. Fracture energy of composites.

Table 2. Fracture energy data from NIST.

Material designation	Al_2O_3content (wt%)	Grain size (µm)	Porosity (%)	Fracture energy (J.m^{-2})
Lucalox[31]	99.9	10	-	18.0
Lucalox-HS[32]	99.9	6-10	-	18.0
AD-999[33]	99.9	3	-	24.3
XA16[34]	99.9	0.53	10	11.7
		0.89	6	26.8
		1.3	5	31.4
		1.9	2.5	25.5
		3.3	5	22.6
		3.7	2.0	36.3
		4.1	5	23.8
		5.0	1.2	36.5
		7.2	1.0	31.1

energy is necessary to break bonds. On the other hand, the roughness should also have contributed to the reduced E values obtained for A_F21 and A_C21. Binns and Popper[32] found energy fracture values of 30 J·m^{-2} (95.6% Al_2O_3 purity, 5-µm grain size, 2% porosity) and 53 J·m^{-2} (97.3% Al_2O_3 purity, 30-µm grain size, 5% porosity). Thus, composites A_F21 and A_C21 could be used for some applications where high impact resistance is required in addition to wear resistance.

Composites A_F7 and A_C7 showed higher flexural strength (FS) values than alumina A_F, A_M, and A_C, as shown in Figure 6. Sathinyakumar and Gnanam[33] obtained 119 MPa for pure alumina sintered at 1400 ºC, while Goswami and Das[34] obtained 288 MPa for LPS alumina, just slightly higher than the highest value found in this study (273 MPa for composite A_F7). With the increase of LZSA content, the FS value decreased, probably due to the increase of the natural defect size (*a*), obtained from Eq. 1, of the composites (Figure 7). By comparison, Figures 6 and 7 show that FS is higher for lower values of natural defect size. Figure 7 shows that *a* increased with the increase of alumina particle size and LZSA content. However, these effects tend to be insignificant at higher LZSA contents (~ 21 vol%). Alumina

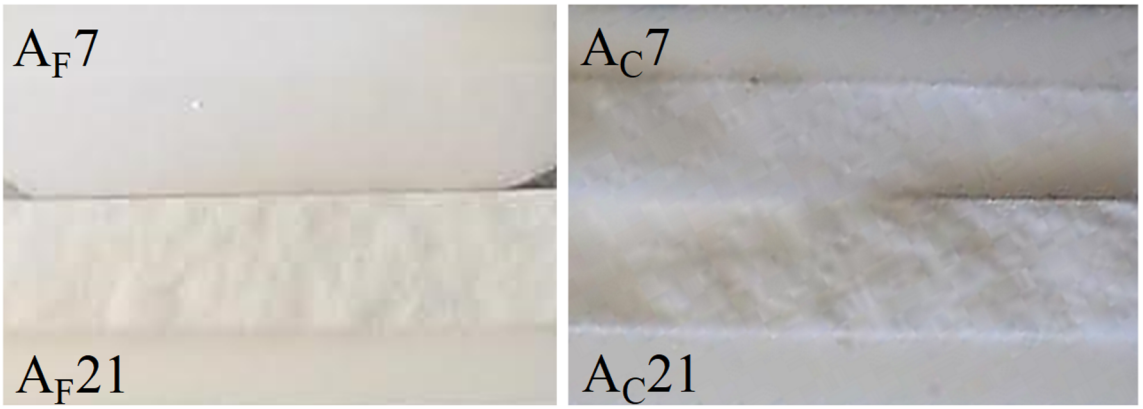

Figure 5. Images (photographies) showing the texture of composites A_F7, A_F21, A_C7 and A_C21.

particle size seems to be the main factor that determined the sizes of the natural defects in the samples with up to 7 vol% LZSA. On the other hand, the addition of 21 vol% LZSA (composites A_F21 and A_C21) increased the natural defect size for all investigated alumina. It is possible that the residual vitreous phase in these composites has increased the natural defect size, as reported by De Noni et al.[35].

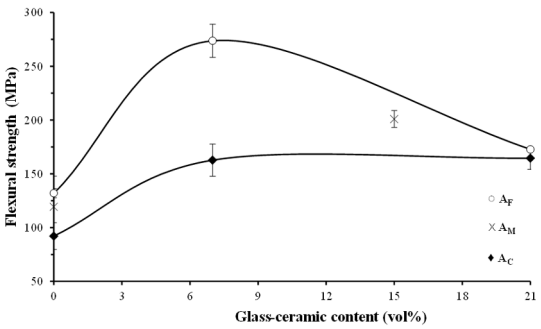

Figure 6. Flexural strength in function of LZSA content of the alumina ceramics and LZSA/alumina composites.

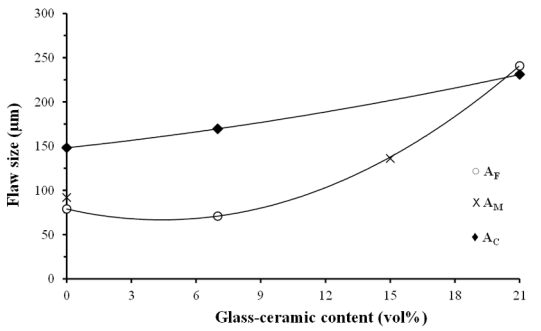

Figure 7. Calculated natural defect size in function of LZSA content of the alumina ceramics and LZSA/alumina composites.

As mentioned before, LZSA glass-ceramic was added to alumina in order to generate residual stress and improve the mechanical properties. Figure 8 presents the XRD patterns of composites A_F, A_F7, and A_F21. Peak displacement occurred toward the left side of the XRD patterns; the higher the LZSA content, the higher the displacement. This displacement demonstrates the existence of compressive residual stresses that were caused by the lower coefficient of thermal expansion of LZSA (5.2×10^{-6} °C^{-1})[20] in comparison to alumina (8.1×10^{-6} °C^{-1}). The other composites also showed the same behavior. Figure 8 also shows that the peak displacement was higher for composite A_F21 than for composite A_C21, possibly due to the greater specific surface area of the former; and consequently, the greater interface region between the alumina and the LZSA. Thus, the interaction between fine alumina (A_F) and the LZSA may help to explain the mechanical behavior of the investigated composites.

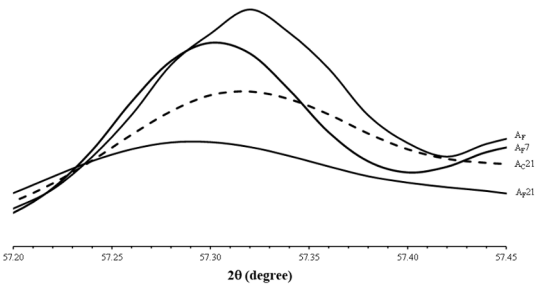

Figure 8. Partial XRD patterns of the alumina A_F and composites A_F7, A_F21 and A_C21.

Figure 9 shows SEM observations of fractured specimens of the alumina ceramics and composites. LZSA is homogeneously dispersed in all the specimens, as detailed in Figure 10. It seems as if the microstructure of composites A_M15 and A_C21 are quite similar, which could explain the similarity in their mechanical properties.

The LZSA addition also changed the morphology of the alumina, as shown in Figure 11 for the etched specimens. The morphology is influenced by the chemical composition of the intergranular phase of materials obtained by LPS and can significantly change the mechanical properties of alumina[36-38]. As shown in the SEM observations, the composites have

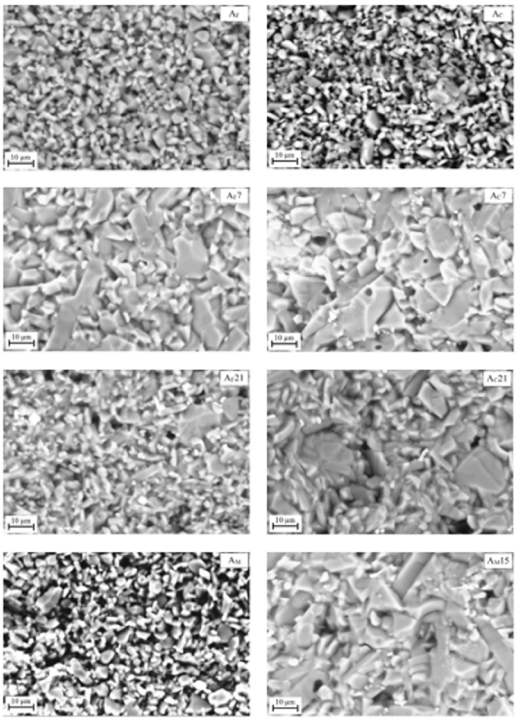

Figure 9. SEM observations of the alumina ceramics and LZSA/alumina composites: fractured specimens.

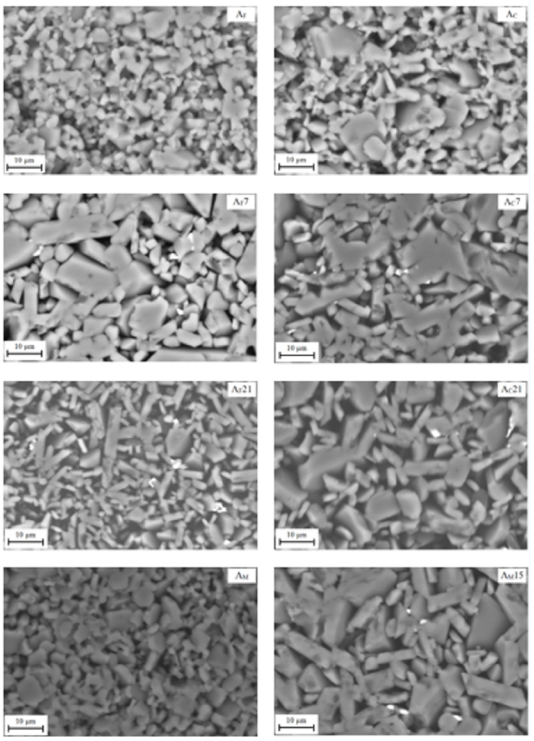

Figure 11. SEM observations of the alumina ceramics and LZSA/alumina composites: etched specimens.

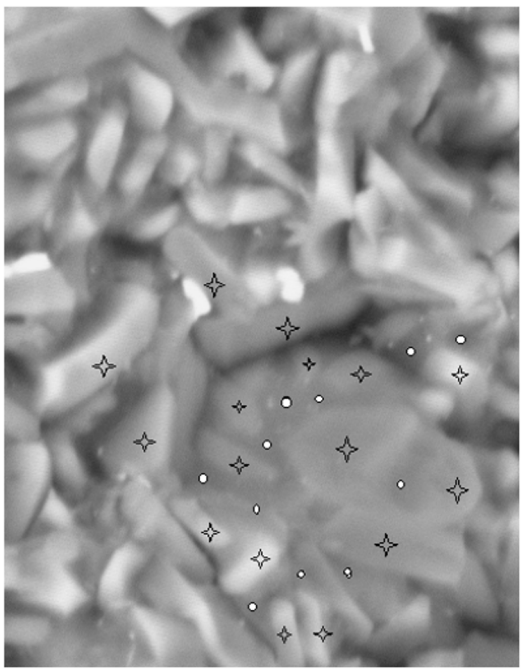

Figure 10. Detail of the fractured composite A_C21: ✧ alumina and ○ LZSA glass-ceramic.

elongated grains. Elongated grains can act as reinforcement material in the microstructure and indeed contribute to the increased fracture toughness[36,38]. Composite A_F21 achieved a high relative density at a lower temperature (1470 °C); and because of this, alumina grains did not experience as much growth. In fact, sintering at lower temperatures in the presence of the liquid phase may cause a suppression of grain growth[38]. Although composites A_F7 and A_C7 show the presence of elongated grains, one can also see coarse, equiaxed grains.

4. Conclusions

The influence of LZSA (Li_2O-ZrO_2-SiO_2-Al_2O_3) glass-ceramic on the mechanical behavior of alumina was investigated. Liquid phase sintering promoted higher densification than the use of pure alumina. A composite containing fine grain alumina and 21 vol% of glass-ceramic sintered at 1470 ºC (3 h holding time) showed lower porosity (2%) than pure alumina sintered at 1600 °C (5%). The initial particle size of alumina had little influence on the mechanical properties; however, the glass-ceramic addition caused a significant effect on the mechanical properties. Elongated grains of alumina were observed in the composites as a result of glass-ceramic addition, which caused strengthening of the structure and improved the fracture toughness. Fine-grained alumina-based composite containing 21 vol% of glass-ceramic (1470 ºC and 3 h holding time, 2% porosity) showed a fracture toughness of 4.93 $MPa \cdot m^{0.5}$, elastic modulus of 210 GPa, fracture energy of 57 $J \cdot m^{-2}$, and flexural strength of 170 MPa, in very good agreement with values reported in the literature. Thus, the introduction of a liquid phase in the sintering of alumina,

which crystallizes during controlled cooling, i.e. the use of a glass-ceramic, allowed us to modify significantly the microstructure of alumina, and consequently, the mechanical properties. The results showed that the addition of the LZSA glass-ceramic improved the mechanical properties of alumina.

5. Acknowledgements

The authors are very grateful to Conselho Nacional de Desenvolvimento Científico e Tecnológico (CNPq/Brazil) and Financiadora de Estudos e Projetos (FINEP/Brazil) for funding this study.

6. References

1. Medvedovski E. Wear-resistant engineering ceramics. *Wear*. 2001;249(9):821-828. DOI: 10.1016/S0043-1648(01)00820-1
2. Zhou J, Bahadur S. Erosion characteristics of alumina ceramics at high temperatures. *Wear*. 1995;181-183(Pt 1):178-188. DOI: 10.1016/0043-1648(95)90022-5
3. Zhang Y, Cheng YB, Lathabai S. Erosion of alumina ceramics by air- and water-suspended garnet particles. *Wear*. 2000;240(1-2):40-51. DOI: 10.1016/S0043-1648(00)00335-5
4. Zhang FC, Luo HH, Wang TS, Roberts SG, Todd RI. Influence factors on wear resistance of two alumina matrix composites. *Wear*. 2008;265(1-2):27-33. DOI: 10.1016/j.wear.2007.08.011
5. Puchy V, Hvizdos P, Dusza J, Kovac F, Inam F, Reece MJ. Wear resistance of Al_2O_3-CNT ceramic nanocomposites at room and high temperatures. *Ceramics International*. 2013;39(5):5821-5826. DOI: 10.1016/j.ceramint.2012.12.100
6. Cesari F, Esposito L, Furgiuele FM, Maletta C, Tucci A. Fracture thoughness of alumina-zirconia composites. *Ceramics International*. 2006;32(3):249-255. DOI: 10.1016/j.ceramint.2005.02.012
7. Medvedovski E. Alumina-mullite ceramics for structural applications. *Ceramics International*. 2006;32(4):369-375. DOI: 10.1016/j.ceramint.2005.04.001
8. Silva MV, Stainer D, Al-Qureshi HA, Montedo ORK, Hotza D. Alumina-Based Ceramics for Armor Application: Mechanical Characterization and Ballistic Testing. *Journal of Ceramics*. 2014;2014:618154. DOI: 10.1155/2014/618154
9. Kumar AS, Durai AR, Sornakumar T. Wear behaviour of alumina based ceramic cutting tools on machining steels. *Tribology International*. 2006;39(3):191-197. DOI: 10.1016/j.triboint.2005.01.021
10. Cho SJ, Hockey BJ, Lawn BR, Bennison SJ. Grain-Size and R-Curve Effects in the Abrasive Wear of Alumina. *Journal of the American Ceramic Society*. 1989;72(7):1249-1252. DOI: 10.1111/j.1151-2916.1989.tb09718.x
11. Mukhopadhyay AK, Mai YW. Grain size effect on abrasive wear mechanisms in alumina ceramics. *Wear*. 1993;162-164(Pt A):258-268. DOI: 10.1016/0043-1648(93)90508-J
12. Miranda-Martinez M, Davidge RW, Riley FL. Grain size effects on the wet erosive wear of high-purity polycrystalline alumina. *Wear*. 1994;172(1):41-48. DOI: 10.1016/0043-1648(94)90297-6
13. Davidge RW, Riley FL. Grain-size dependence of the wear of alumina. *Wear*. 1995;186-187(Pt 1):45-49. DOI: 10.1016/0043-1648(95)07171-7
14. Galusek D, Twigg PC, Riley FL. Wet erosion of liquid phase sintered alumina. *Wear*. 1999;233-235:588-595. DOI: 10.1016/S0043-1648(99)00236-7
15. Krell A, Blank P, Ma H, Hutzler T, Nebelung M. Processing of High-Density Submicrometer Al2O3 for New Applications. *Journal of the American Ceramic Society*. 2003;86(4):546-553. DOI: 10.1111/j.1151-2916.2003.tb03339.x
16. Roy RS, Guchhait H, Chanda A, Basu D, Mitra MK. Improved sliding wear-resistance of alumina with sub-micron grain size: A comparison with coarser grained material. *Journal of the European Ceramic Society*. 2007;27(16):4737-4743. DOI: 10.1016/j.jeurceramsoc.2007.02.205
17. Hsu YF, Wang SF, Wang YR, Chen SC. Effect of niobium doping on the densification and grain growth in alumina. *Ceramics International*. 2008;34(5):1183-1187. DOI: 10.1016/j.ceramint.2007.02.010
18. Wu Y, Zhang Y, Choy KL, Guo J. Liquid-phase sintering of alumina with YSiAlON oxynitride glass. *Materials Letters*. 2003;57(22-23):3521-3525. DOI: 10.1016/S0167-577X(03)00119-8
19. Montedo ORK, Milak PC, Minatto FD, Nuernberg RB, Faller CA, Oliveira APN, et al. Effect of a LZSA glass-ceramic addition on the sintering behavior of alumina. *Journal of Thermal Analysis and Calorimetry*. 2016;124(1):241-249. DOI: 10.1007/s10973-015-5144-5
20. Montedo ORK, Bertan FM, Piccoli R, Hotza D, Klein AN, Oliveira APN. Low thermal expansion sintered LZSA glass-ceramics. *American Ceramic Society Bulletin*. 2008;87:34-38.
21. Montedo ORK, Floriano FJ, de Oliveira Filho J, Angioletto E, Bernardin AM. Sintering behavior of LZSA glass-ceramics. *Materials Research*. 2009;12(2):197-200. DOI: 10.1590/S1516-14392009000200014
22. Montedo ORK, Floriano FJ, de Oliveira Filho J. Sintering kinetics of a $18.8Li_2O$ $8.3ZrO_2$ $64.2SiO_2$ $8.7Al_2O_3$ glass ceramic. *Ceramics International*. 2011;37(6):1865-1871. DOI: 10.1016/j.ceramint.2011.03.047
23. Montedo ORK, Oliveira APN. Relationship between Surface Abrasion Wear and Brightness in Glazed Porcelainized Stoneware Tiles. *ISRN Ceramics*. 2011;2011:548129. DOI: 10.5402/2011/548129
24. Montedo ORK, Hotza D, Oliveira APN, Meszaros R, Travitzky N, Greil P. Crystallisation Kinetics of a ß-Spodumene-Based Glass Ceramic. *Advances in Materials Science and Engineering*. 2012;2012:525428. DOI: 10.1155/2012/525428
25. Montedo ORK, Milak PC, Faller CA, Peterson M, Angioletto E, De Noni A Jr. Effect of LZSA Glass-Ceramic Addition on the Pressureless Sintered Alumina. Part I: Grain Growth. *Materials Research*. 2017;20(4):1024-1028. DOI: 10.1590/1980-5373-mr-2016-0964
26. Terheci M. Grain boundary and testing procedure, a new approach to the tribology of alumina materials. *Wear*. 1997;211(2):289-301. DOI: 10.1016/S0043-1648(07)00133-0

27. Munro M. Evaluated Material Properties for a Sintered alpha-Alumina. *Journal of the American Ceramic Society*. 1997;80(8):1919-1928. DOI: 10.1111/j.1151-2916.1997.tb03074.x

28. Lube T, Pascual J, Chalvet F, Portu G. Effective fracture toughness in Al_2O_3-Al_2O_3/ZrO_2 laminates. *Journal of the European Ceramic Society*. 2007;27(2-3):1449-1453. DOI: 10.1016/j.jeurceramsoc.2006.04.063

29. Marques CM. Relação entre microestrutura e desgaste erosivo a frio e a quente em materiais cerâmicos à base de alumina. [PhD Thesis]. Porto Alegre: Universidade Federal do Rio Grande do Sul; 2006.

30. Tuan WH, Lai MJ, Lin MC, Chan CC, Chiu SC. The mechanical performance of alumina as a function of grain size. *Materials Chemistry and Physics*. 1994;36(3-4):246-251. DOI: 10.1016/0254-0584(94)90037-X

31. *National Institute of Standards and Technology* - NIST. Available from: <http://www.nist.gov/>. Access in: 04/10/2017.

32. Binns DB, Popper P. Mechanical Properties of Some Commercial Alumina Ceramics. *Proceedings of the British Ceramic Society*. 1966;122:71-82.

33. Sathiyakumar M, Gnanam FD. Role of wollastonite additive on density, microstructure and mechanical properties of alumina. *Ceramics International*. 2003;29(8):869-873. DOI: 10.1016/S0272-8842(03)00029-4

34. Goswami AP, Das GC. Role of fabrication route and sintering on wear and mechanical properties of liquid-phase-sintered alumina. *Ceramics International*. 2000;26(8):807-819. DOI: 10.1016/S0272-8842(00)00022-5

35. De Noni A Jr., Hotza D, Soler VC, Vilches ES. Influence of composition on mechanical behaviour of porcelain tile. Part III: Effect of the cooling rate of the firing cycle. *Materials Science and Engineering: A*. 2011;528(9):3330-3336. DOI: 10.1016/j.msea.2010.12.086

36. Goswami AP, Roy S, Mitra MK, Das GC. Influence of powder, chemistry and intergranular phases on the wear resistance of liquid-phase-sintered Al_2O_3. *Wear*. 2000;244(1-2):1-14. DOI: 10.1016/S0043-1648(00)00407-5

37. Goswami AP, Roy S, Mitra MK, Das GC. Microstructure dependent hardness and fracture behavior in liquid-phase-sintered Al_2O_3. *Ceramics International*. 2000;26(4):397-410. DOI: 10.1016/S0272-8842(99)00070-X

38. Goswami AP, Roy S, Mitra MK, Das GC. Impurity-Dependent Morphology and Grain Growth in Liquid-Phase-Sintered Alumina. *Journal of the American Ceramic Society*. 2001;84(7):1620-1626. DOI: 10.1111/j.1151-2916.2001.tb00886.x